Stoichiometric analysis of oligomerization of membrane proteins using coiled-coil labeling and in-cell spectroscopy(Digest_要約)

AUTHOR(S):

Kawano, Kenichi

Stoichiometric analysis of oligomerization of membrane proteins using coiled-coil labeling and in-cell spectroscopy

（新規小分子ラベル法と in-cell 蛍光分光法を用いた
膜タンパク質の会合状態の定量的解析）

2013

Kenichi Kawano

Stoichiometric analysis of oligomerization of membrane proteins using coiled-coil labeling and in-cell spectroscopy

（新規小分子ラベル法と in-cell 蛍光分光法を用いた
膜タンパク質の会合状態の定量的解析）

A doctoral thesis submitted to Graduate School of Pharmaceutical Sciences, Kyoto University

2013

Kenichi Kawano

Contents

Abbreviations

Alexa568	Alexa Fluor 568 (FRET donor dye)
Alexa647	Alexa Fluor 647 (FRET acceptor dye)
Am	amantadine hydrochloride
β_2AR	β_2-adrenergic receptor
BRET	bioluminescence resonance energy transfer
CHO	chinese hamster ovary
DMF	*N*, *N*-dimethylformamide
DMSO	dimethylsulfoxide
E3	$(EIAALKE)_3$
FRET	fluorescence resonance energy transfer
GpA*	glycophorin A G83I mutant
GPCR	G-protein coupled receptor
GFP	green fluorescent protein
HEK	human embryonic kidney
K4	$(KIAALEK)_4$
M2	influenza virus A M2 ion channel
MALDI-MS	matrix-assisted laser desorption-ionization mass spectrometry
mGluR	metabotropic glutamate receptor
PBS(+)	phosphate-buffered saline (PBS) containing 0.33 mM $MgCl_2$ and 0.90 mM $CaCl_2$

Symbols

E	true FRET efficiency
E_{app}	apparent FRET efficiency
R_0	Förster distance
$R_{561/637}$	the ratio of fluorescence intensities of the acceptor (Alexa568-K4) excited at 561 nm and 637 nm
X_D	donor mole fraction

Chapter 1

Establishment of stoichiometric analysis for oligomerization of membrane proteins in the plasma membrane of living cells.

1.1 Introduction

Many membrane proteins are proposed to work as oligomers, including association between the same subtypes (homooligomerization) or of different subtypes (heterooligomerization), for faster signaling, specific crosstalks or responses, and ionic transport[1]. The oligomerization of membrane proteins has been detected with destructive[2,3] or nondestructive methods[4,5,6].

The existing methodologies, however, are not suitable to precisely determine the oligomeric states of membrane proteins in living cells. The destructive methods such as immunoprecipitation can detect artificial aggregation of proteins after detergent solubilization. Fluorescence and bioluminescence resonance energy transfer (FRET and BRET) have been widely used as a nondestructive indicator of interaction among target proteins in living cells. Although most studies use fluorescent proteins or luminescent proteins to label the target proteins, these methods have limitations for the quantitative analysis of protein oligomerization: (*i*) the detection of signals from not only surface receptors but also intracellular receptors; (*ii*) the difficulty in controlling the donor / acceptor expression ratios; (*iii*) the perturbation of protein functions due to the considerable size of the label. Therefore, cell-surface-specific labeling, accurate control of the labeling stoichiometry of the energy donor and acceptor, and downsizing of the label should significantly improve the reliability of analysis. Posttranslational labeling methods using a genetic tag and a synthetic probe are promising to fulfill these requirements[7,8].

Here I show that a combination of the coiled-coil tag–probe labeling method[9] and spectral imaging enabled a stoichiometirc analysis of oligomeric state of membrane proteins on living cells using monomeric, dimeric, and tetrameric standard membrane proteins.

1.2 Materials and Methods

Vector construct.

cDNA encoding E3-GpA was inserted into pcDNA3 for transient expression as follows. The gene of human GpA, which had a *Hind*III site at the 5'-terminus and a *Xba*I site at the 3'-terminus, was amplified by PCR from human GpA / pDNR-LIB (Open Biosystems, Huntsville, US). The PCR product was digested with *Hind*III and *Xba*I and inserted into the *Hind*III and *Xba*I site of pcDNA3. Oligo DNA encoding E3-tag (Life Technology, Carlsbad, US), edges of which had *Bst*XI sites, was digested and inserted into a *Bst*XI site (G24−V25) at the N-terminus of GpA / pcDNA3. Gly83 of E3-GpA / pcDNA3 was then mutated to Ile by using a Quickchange site-directed mutagenesis kit (Stratagene, San Diego, US) to obtain E3-GpA* / pcDNA3. cDNA encoding E3-mGluR1b was inserted into the pcDNA3 vector as follows. A *Cla*I site (1894−1899 bp) in the mGluR1 sequence of mouse mGluR1 / pYX (Open Biosystems, Huntsville, US) was abolished by silent mutation using the Quickchange site-directed mutagenesis kit (Stratagene, San Diego, US). The gene of mGluR1, which had a *Cla*I site at the 5'-terminus and a *Nhe*I site at the 3'-terminus, was amplified by PCR from the point-mutated mGluR1 / pYX vector. The PCR product and E3-EGFR / pcDNA3 were digested with *Cla*I and *Nhe*I. The DNA for mGluR1 was then inserted into the vector DNA (E3 / pcDNA3) to obtain an E3-mGluR1 / pcDNA3 vector. cDNA encoding E3-M2 was inserted into pcDNA3 as follows. Oligo DNA encoding M2 of influenza virus A (A_Udorn_1972 (H3N2)) (Genscript, Inc., Piscataway, US), which had a *Nhe*I site at the 5'-terminus and an *Apa*I site at the 3'-terminus, was digested with *Nhe*I and *Apa*I. The DNA of M2 was inserted into the vector DNA (E3 / pcDNA3 from E3-EP3β / pcDNA3 vector) to obtain an E3-M2 / pcDNA3 vector.

Cell culture and transfection.

CHO-K1 cells (ATCC, Manassas, US) were used for transient expression of membrane proteins. The cells were cultured in Ham's F12 medium (Life Technology, Carlsbad, US) supplemented with 10% FBS, L-glutamine and antibiotics of penicillin at 50 units / mL and streptomycin at 50 μg / mL (Nacalai Tesque, Kyoto, Japan) at 37°C in a 5% CO_2 incubator (Sanyo Electric Co., Ltd., Osaka, Japan).

For the transient expression, CHO-K1 cells were seeded at 1.0×10^5 in a 35-mm glass bottom dish ((Advanced TC treated), Greiner bio-one, Kremsmüenster, Austria). The medium of cells was changed to a serum-free medium and the cells were incubated with a transfection mixture composed of 2.0 μg of DNA, 4.0 μL of Lipofectamine LTX (Life Technology, Carlsbad, US), and 400 μL of Opti-MEM (Life Technology, Carlsbad, US) per dish at 30 h from seeding. The medium was changed to a fresh medium containing 10% FBS at 5 h from transfection. CHO-K1 cells were imaged at

18 h from transfection. For transfection of E3-mGluR1b, the transfection mixture was composed of 2.0 μg of DNA, 8.0 μL of Lipofectamine LTX, 2.0 μL of PLUS reagent (Life Technology, Carlsbad, US), and 400 μL of Opti-MEM per dish.

Peptide synthesis

The K4 peptide $(KIAALKE)_4$ was synthesized by a standard 9-fluorenylmethyloxycarbonyl (Fmoc)-based solid-phase method using NovaSyn TGR resin (Novabiochem, Läufelfingen, Switzerland). For coupling, Fmoc amino acid (0.5 mmol), 1-hydroxybenzotriazole (0.5 mmol), and *N*-*N*'-diisopropylcarbodiimide (0.5 mmol) dissolved in *N*, *N*-dimethylformamide ((DMF), Wako, Saitama, Japan) were reacted for 2 h. The reaction was monitored using the ninhydrin test. Fmoc was removed by treatment with 20% piperidine in DMF for 20 min. The peptides were separately labeled at the N-terminus with 0.2–0.3-equivalent Alexa Fluor 568 and Alexa Fluor 647 succinimidyl ester (Life Technology, Carlsbad, US) in DMF containing 5% *N*, *N*-diisopropylethylamine for 48 h to produce Alexa568-K4 and Alexa647-K4, respectively. The peptide was removed from the resin by treatment with TFA / ethaneditiol / *m*-cresol / thioanisole / H_2O = 12.5 / 1 / 1 / 1 / 1 (v / v) for 3 h, precipitated by diethylether, and purified by reversed phase HPLC. The purity of the synthesized peptides (higher than 95%) was determined by analytical HPLC and matrix-assisted laser desorption-ionization mass spectrometry ((MALDI-MS), Shimadzu, Kyoto, Japan).

Determination of concentrations and extinction coefficients at 561 nm of Alexa568-K4 and Alexa647-K4.

Freeze-dried Alexa568-K4 and Alexa647-K4 peptides were dissolved in 200 μl highly pure water (Merck Millipore, Billerica, US). The extinction coefficients of Alexa Fluor 568 and 647 (Life Technology, Carlsbad, US) are reported to be 88,000 (578 nm) in aqueous buffer at pH 7 and 270,000 (651 nm) in MeOH, respectively. Therefore, Alexa568-K4 and Alexa647-K4 peptides were diluted by 1 / 32 (3.13%) in aqueous buffer and MeOH, respectively, and the concentrations of the peptides were determined using an UV-visible spectrophotometer (Shimadzu, Kyoto, Japan) based on the respective maximum absorbance at 25°C. The extinction coefficients at 561 nm of Alexa568-K4 (ε_D (λ_{561})) and Alexa647-K4 (ε_A (λ_{561})) for determination of E_{app} values were also calculated from the ratio of absorbance at 561 nm to the respective maximum values.

Labeling E3-tagged proteins with K4 probes for examining self-association.

The mixtures of Alexa568-K4 and Alexa647-K4 probes were diluted with phosphate-buffered saline (PBS) containing 0.33 mM $MgCl_2$ and 0.90 mM $CaCl_2$ (PBS

(+)) to produce 50 nM K4 probe solutions (1 mL). The solutions were added to cells to label the E3-tagged proteins for 5 min.

Confocal microscopy.

All imaging experiments were performed using a confocal microscope (Nikon C1, Tokyo, Japan) under a water-immersed 60× objective (Plan Apo VC) with 561 nm and 637 nm lasers. To examine the self-association of membrane proteins, spectral images were obtained with a spectrum detector. Spectra in the range of 565 to 745 nm (resolution: 10 nm) were acquired. For other experiments, confocal images were obtained with a standard detector through a BP575−615 nm emission filter for the donor and a LP650 nm emission filter for the acceptor.

Analysis of E_{app} values.

E3-tagged membrane proteins on cell surfaces were labeled with K4 probes at various X_D values, and excited at 561 nm to obtain fluorescence emission spectra from cell membranes. No nonspecific binding of K4 probes was observed on the plasma membranes of mock-transfected cells. Although the observed spectra included background fluorescence due to free probes (< 10% of signals), it did not affect the quantification because it was subtracted before data analysis. For deconvolution of the observed spectra into donor and acceptor spectra, I separately obtained the reference spectra of the donor excited at 561 nm and acceptor excited at 637 nm from the proteins labeled with either the donor or the acceptor K4 probes. The E_{app} values were calculated with the equation

$$E_{app} = \frac{\varepsilon_A(\lambda_D{}^{ex})}{\varepsilon_D(\lambda_D{}^{ex})} \times \left(\frac{F_{AD} - F_A}{F_A} \right) \qquad \text{[Eq. 1]}$$

where E_{app} denotes the apparent FRET efficiency based on sensitized acceptor emission, ε_A ($\lambda_D{}^{ex}$) and ε_D ($\lambda_D{}^{ex}$) represent the molar extinction coefficent of the acceptor and donor at 561 nm, respectively, F_{AD} and F_A indicate the acceptor emission (arbitrary unit) excited at 561 nm in the presence and absence of the donor, respectively[10]. However, F_A cannot be directly acquired in the presence of the donor. I, therefore, measured the ratio of fluorescence intensities of the acceptor excited at 561 nm and 637 nm ($R_{561\,/\,637}$) from E3-tagged membrane proteins labeled with the acceptor, and multiplied the fluorescence intensity of the acceptor acquired by exciting at 637 nm in the presence of the donor by the $R_{561/637}$ ratio to obtain the F_A value.

Spectral deconvolution with least-squares method.

I determined the E_{app} values on an Excel data sheet (Microsoft, Redmond, US) using a least-squares method. Deconvolution of observed spectra (ex. 561 nm) into donor and acceptor spectra was performed by minimizing

$S_1 = \sum_{\lambda}\left[\left(f_1 \times d_R(\lambda) + f_2 \times a_R(\lambda)\right) - S_{obs(561)}(\lambda)\right]^2$, where $d_R(\lambda)$, $a_R(\lambda)$, and $S_{obs(561)}(\lambda)$ represent the fluorescence intensity of the donor and acceptor, and the observed fluorescence intensity at each wavelength λ (ex. 561 nm), and the wavelength-independent adjustable parameters f_1 and f_2 denote contributions of the donor and acceptor, respectively. Fitting of observed spectra excited at 637 nm ($S_{obs(637)}(\lambda)$) to acceptor spectra was performed by minimizing the S_2 value in the equation $S_2 = \sum_{\lambda}\left(f_3 \times a_R(\lambda) - S_{obs(637)}(\lambda)\right)^2$. The F_{AD} / F_A value in Eq. 1 was calculated as $\frac{f_2}{R_{561/637} \times f_3}$.

Theoretical curves.

The theoretical curve is given as

$$E_{app} = E \times \frac{X_D}{1 - X_D} \times [1 - \{X_D(1 - X'_U) + X'_U\}^{N-1}] \qquad \text{[Eq. 2]}$$

where X_D, X'_U, and N indicate the donor molar fraction, the unlabeled receptors fraction, and the association number, respectively[10]. In the present study, the X'_U value was estimated to be 0.1 according to occupancies (~90%) of E3-tagged membrane proteins labeled with K4 probes at 50 nM (see Eq. 3). E represents true FRET efficiency in the oligomers and is determined by the distance and the mutual orientation of the donor and acceptor. The assumption of a random orientation of the fluorophores[11] is reasonable because the probes were attached in the flexible N-terminal regions.

Binding assay for K4 probes.

The cells were seeded at 3.0×10^5 cells in a 35-mm glass bottom dish, and labeled with Alexa568-K4 or Alexa647-K4 at concentrations of 5, 10, 20, and 100 nM at 24 h from seeding. After incubation for 10 min, confocal images were acquired by using a laser scanning confocal microscope to obtain the fluorescence intensity of cell surface. The background fluorescence due to free probes (< 10% of signals) was subtracted before data analysis. K_d values of K4 probes and occupancies of E3-tagged proteins labeled with K4 probes were determined as

$$[R] = [R]_{total} \times \frac{[P]_{free}}{[P]_{free} + K_d} \qquad \text{[Eq. 3]}$$

where [R] denotes the amount of K4 probe-bound proteins, $[R]_{total}$ indicates the amount of total proteins on cell surface and equals to the maximal binding which is approached asymptotically in the saturation curves, $[P]_{free}$ is the free concentration of K4 probes, and K_d is the dissociation constant[12]. The occupancies of proteins labeled with K4 probes ($[R]/[R]_{total}$) were calculated by using Eq. 3.

1.3 Results

Coiled-coil tag−probe labeling method.

The coiled-coil tag−probe labeling method[9] utilizes tight interaction between the heterodimeric coiled-coil peptides E3 $(EIAALEK)_3$ and K4 $(KIAALKE)_4$. These peptides have net negative charges (−3) and positive charges (+4), respectively. In addition to electrostatic interaction between E and K, hydrophobic interaction between L and I drives the formation of a heterodimer of E3 and K4 (**Fig. 1-1A**). The E3 peptides were genetically tagged to the N-termini of target membrane proteins, whereas the K4 probes were chemically synthesized and labeled at their N-termini with either the donor dye Alexa Fluor 568 or the acceptor dye Alexa Fluor 647 to obtain Alexa568-K4 (donor) or Alexa647-K4 (acceptor), respectively (**Fig. 1-2A**). The addition of the K4 probes can label the E3-tagged receptors expressed on living cells within 1 min[9].

This labeling method has many advantages for measurements of the oligomerization of cell-surface proteins: (*i*) the K4 probes label receptors only on cell membranes because of their membrane impermeability (**Figs. 1-2B and C**), (*ii*) the E3-tagged receptors can be labeled with multicolor K4 probes at the same time by addition of a mixture of probes, (*iii*) the ratio of donor to acceptor is controllable, and (*iv*) perturbation of receptor function can be minimized due to the small size of E3 and K4 (the total size is 5−6 kDa, which is one fifth of green fluorescent proteins (GFP)).

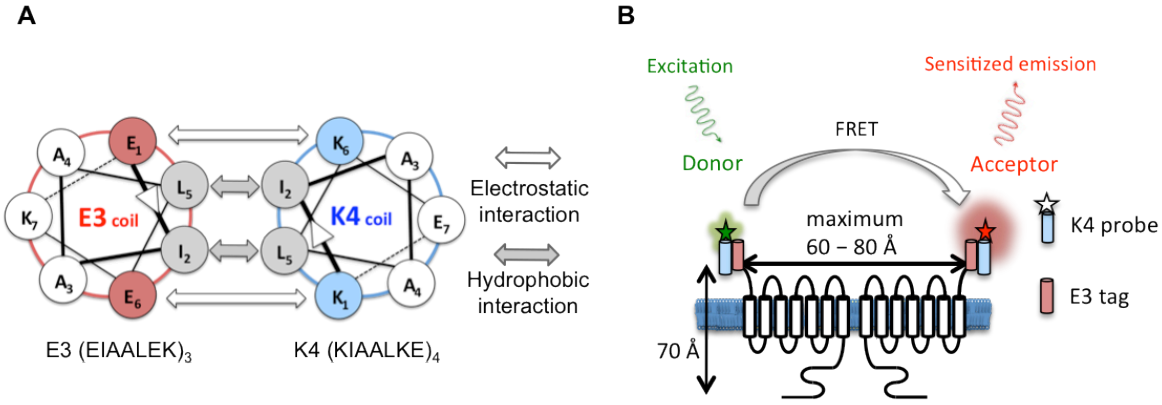

Figure 1-1. Coiled-coil tag–probe labeling method and schematic diagram of FRET within a GPCR dimer. (A) Helical wheel representation of the E3 and K4 heterodimer. The peptide chains propagate into the page from the N-terminus to the C-terminus. Gray and white double-headed arrows show hydrophobic interaction between the side chains of L and I in a "knobs-into-holes" manner and electrostatic interaction between the side chains of E and K, respectively. (B) Schematic diagram of FRET within a GPCR dimer. Green and red stars show the energy donor fluorophore (Alexa568) and energy acceptor fluorophore (Alexa647), respectively. Red and blue cylinders show E3 tags and K4 probes, respectively.

Alexa568-K4 and Alexa647-K4 have high affinity for E3-tagged receptors with dissociation constants (K_d) of ~5 nM (**Figs. 1-2 D and E**); these values are consistent with previously reported K_d of ~6 nM, for example the tetramethylrodamine-labeled K4 probe, and much greater than K_d of ~64 nM for the K3 probes[9] (in vitro, *de novo* E3–K3 coiled-coil complex is a remarkably stable heterodimer, with a denaturation point of 4.3 M GdnHCl, K_d of 70 nM, and a $\Delta G^{H_2O} = -9.6$ kcal / mol[13]). The high affinity enables to reduce the background signals (< 10% compared with the membranes) because the K4 probes can label ~90% of E3-tagged proteins on the cell surface at a mere concentration of 50 nM. The Förster distance (R_0) of this pair (82 Å) covers the maximal plausible distance between the N-termini of a G-protein-coupled receptors (GPCRs) dimer (60−80 Å)[14] (**Fig. 1-1B**).

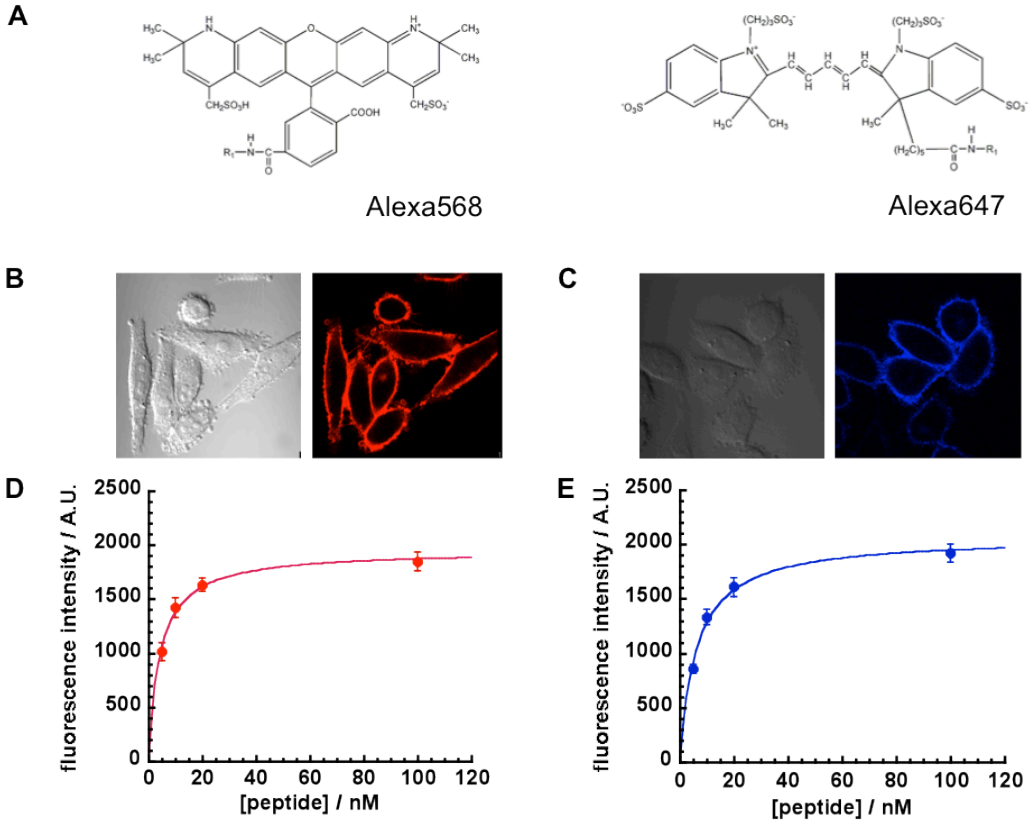

Figure 1-2. Binding assay for K4 probes. Chemical structures of Alexa568 and 647 (A). Confocal images of E3-tagged protein stably-expressing CHO cells labeled with Alexa568-K4 (B) or Alexa647-K4 (C) at a concentration of 5 nM, respectively. The left and right photographs show differential interference contrast images and fluorescence images (512 × 512 pixels) of living cells attached on a glass-bottom dish, respectively. K4 probes were nonspecifically bound to dead cells (< 3%), although they were not included in the analysis. The net fluorescence intensity (the region of interest) is obtained from the plasma membrane region of one cell after subtracting the background signals, and plotted as a function of Alexa568-K4 (D) and Alexa647-K4 (E) concentration. Fluorescence intensity in the y-axis is the average intensity per pixel. Error bars represent mean ± s.e.m., n = 10 (cells). The K_d values of Alexa568-K4 (4.2 ± 0.5 nM) and Alexa647-K4 (6.2 ± 0.9 nM) were determined by fitting the data with Eq. 3. The occupancies of E3-tagged proteins labeled with Alexa568-K4 and Alexa647-K4 were 92.3% and 89.0% at 50 nM, respectively.

Demonstration of stoichiometric analysis with standard membrane proteins.

The theory of a quantitative FRET analysis based on sensitized emissions of the acceptor, which is useful for analysis in living cell membranes, has been previously reported[10], although the reliability has not been tested by using standard membrane proteins with known oligomeric states. Therefore, I initially examined whether the combination of the labeling and analysis methods could determine the oligomeric state of membrane proteins using influenza virus A M2 ion channel (M2) (tetramer)[15], metabotropic glutamate receptor (mGluR) (dimer)[7,16] and glycophorin A G83I mutant (GpA*) (monomer)[17] as standards. The E3-tagged membrane proteins, E3-M2, E3-mGluR1b, and E3-GpA*, were transfected into chinese hamster ovary (CHO) cells, and then labeled with Alexa568-K4 and Alexa647-K4 probes mixed at various donor mole fractions (X_D). Without washout of free probes, the donor fluorophores was excited at 561 nm to obtain fluorescence spectra from regions all over the plasma membranes by using a laser scanning confocal microscope equipped with a spectrum detector. Although the observed spectra included background fluorescence due to free probes (< 10% of signals), it did not affect the quantification because it was subtracted before data analysis. The observed spectra were a composite of emissions from both the donor and the acceptor, and the latter originated from sensitized emission due to FRET and emission from directly excited acceptor at 561 nm. To quantify the sensitized emission, I firstly deconvoluted the observed spectra into spectra of the donor and the acceptor to obtain the total acceptor emission. Next, emission due to direct accepter excitation at 561 nm was calculated by multiplying the fluorescence intensity of the acceptor excited at 637 nm in the presence of the donor by the constant $R_{561/637}$, the ratio of fluorescence intensities of the acceptor excited at 561 nm and 637 nm. **Figure 1-3A** shows the images and spectra of E3-GpA* and E3-M2 labeled with K4 probes at 50 nM and X_D = 0.50 as examples. The spectrum for M2 included significant sensitized emission of the acceptor, indicating the occurrence of FRET, whereas that for GpA* exhibited only weak emissions from the acceptor, which essentially originated from direct excitation, showing the absence of FRET.

Apparent FRET efficiency (E_{app}) was calculated according to Eq. 1. I analyzed E_{app} values as a function of X_D to estimate the stoichiometry of self-association (**Fig. 1-3B**). Based on Eq. 2, the theoretical curve for the monomer remains zero regardless of X_D, and that for the dimer shows a straight line converging to 0.9 at X_D = 1. Curves for higher-order oligomers are concave upward. Measured E_{app} values for the standard membrane proteins could be well explained by corresponding theoretical curves, demonstrating that the oligomeric states of membrane proteins can be correctly determined by using the coiled-coil tag−probe labeling method. Note that random energy transfer was not detected for the monomeric standard protein GpA*, even though its expression level appeared to be more than 5 times higher than those of other standard proteins, based on fluorescence intensity (data not shown).

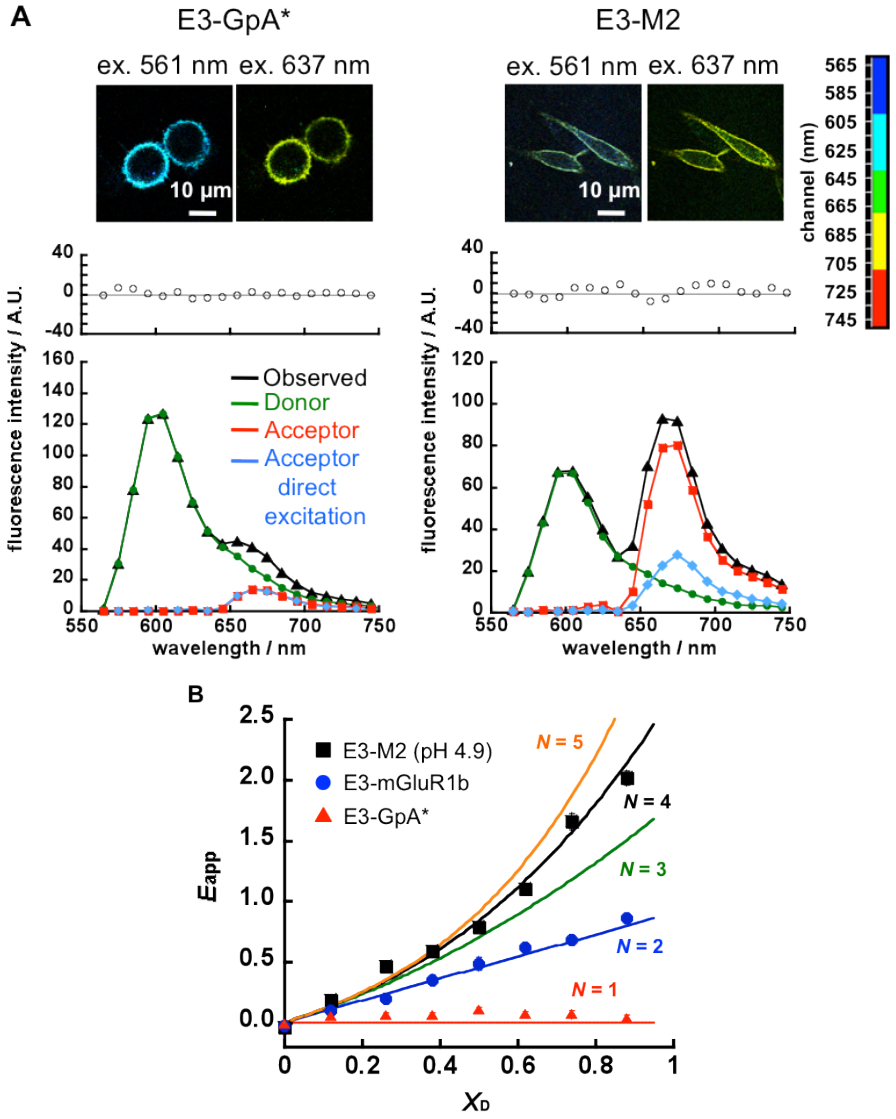

Figure 1-3. Detection of the oligomerization of standard membrane proteins by coiled-coil tag—probe labeling. (A) Spectral images and fluorescence emission spectra of the cell membrane region obtained from E3-GpA* and E3-M2 transiently expressed on CHO cells labeled with K4 probes at X_D = 0.50. Images acquired using a spectrum detector are shown in pseudo-color including spectral information (the scale bar on the right). These images are composite of 19 channels in the range of 565 to 745 nm (resolution: 10 nm). In the spectra for GpA* and M2, black, green, red, and blue lines show the observed spectra, the deconvoluted spectral components of the donor, that of the acceptor, and the spectra expected for directly excited acceptors at 561 nm, respectively. Middle panels show the residuals between the observed and calculated spectra. (B) Determination of oligomeric states. The apparent FRET efficiency, E_{app}, is plotted as a function of the donor mole fraction, X_D. Red, blue, green, black, and orange lines show theoretical curves calculated from [Eq. (2)] for the monomer (N = 1), dimer (N = 2), trimer (N = 3), tetramer (N = 4), and pentamer (N = 5) as a function of X_D, respectively. Triangle, circle, and square symbols represent the measured E_{app} values for E3-GpA* (pH 7.4), E3-mGluR1b (pH 7.4), and E3-M2 (pH 4.9), respectively. Error bars represent the mean ± s.e.m., n = 10.

1.4 Discussion

Recently, new methods based on various detection principles have been developed. For example, fluorescence correlation spectroscopy and photon counting histogram have been applied to determine the brightness of diffusing objects, which is proportional to the number of GPCRs moving together, in living cells[18]. Single-molecule imaging methods were also reported to determine the number of subunits in membrane proteins by counting discrete steps of photobleaching[19], or to monitor the association−dissociation dynamics by single-particle tracking[20,21]. These methods require only single-color-labeled proteins, however, it is difficult to distinguish whether the membrane proteins form oligomers, they exist within the limits of optical resolution (~200 nm), or they are segregated into membrane domains. On the other hand, resonance energy transfer-based methods can detect interaction of membrane proteins when they approach each other within ~10 nm. Although fluorescent or luminescent proteins have been widely used for FRET or BRET methods[4,5,6,22,23,24], they have limitations in surface specificity, controlled multicolor labeling, and size. Another strategy using fluorescent proteins is bimolecular fluoresce complementation[18,22], however, it provides information of the interaction between the split fluorescent proteins and not stoichiometry of interaction of the target proteins. Thus, it is desired to develop cell-surface specific, smaller, and convenient multicolor labeling methods, such as noncovalent coiled-coil labeling[9], covalent SNAP-tag[7], ACP-tag[8] and NTA-His binding technologies[25].

While the covalent systems are promising tools alternative for conventional methods[7,10,16,20], the coiled-coil labeling has more advantages over them[26,27]; (*i*) short labeling time within 1 min (cf. SNAP-tag: 1 h[7], ACP: > 20 min on living cells[8,10]) enables the precise analysis of oligomeric states of receptors on living cells with minimum influences on internalization of the labeled receptors and surface expression of newly biosynthesized receptors; (*ii*) perturbation of receptor function can be minimized owing to the small size of 5–6 kDa (SNAP-tag: ~18 kDa[7]); and (*iii*) although the extracellular probes unable to be removed by washout to keep the constant labeling efficiency, the high affinity of the K4 probes (K_d ~5 nM) reduces background signals in comparison with the NTA-His binding system (Ni-NTA exhibits K_d values of 1.05 μM and 166 nM for $(His)_6$ and $(His)_{10}$ tag-fused receptors, respectively)[25]. The experimental precision of E_{app} in our method was 10% (n = 10). Regarding the sensitivity, the FRET signals can be detected if more than 20% membrane proteins form oligomers. The analytical accuracy has been proven to be 10% by the result that the measured E_{app} values of the standard proteins were within 10% deviations from corresponding theoretical values. The E_{app} value was not influenced by the temperature (4, 20, 30, and 37°C) (data not shown); however, the affinities of K4 probes

to the E3-tagged proteins may be reduced at strong acidic pH or basic pH because pK_a values of glutamic acid and lysine residues of the α-helical structure in the aqueous condition are reported as ~4.3 and ~10.0, respectively[28,29], although I examined the K_d values for Alexa568-K4 and Alexa647-K4 were not changed between pH 4.9 and 7.3. Additionally, the purity of K4 probe is very important factor for quantitative analysis because the presence of unlabeled probes reduces the apparent labeling efficiency and FRET does not occur between labeled- and unlabeled-probes bound proteins; therefore, E_{app} value may be underestimated even if the target proteins form oligomers. Thanks to being careful about the purities of the probes and pH condition, indeed, our simple experimental procedures and precise analysis enable discrimination of dimer and tetramer without complicated steps. Moreover, the results of mGluR1b demonstrated that this method is applicable for not only class C GPCRs with large extracellular regions forming 'head-to-head' dimers but also class A GPCRs having compact structures and short N-termini.

In summary, I established a new methodology for stoichiometric analysis of the oligomerization of membrane proteins on living cells by using FRET among proteins labeled by the novel coiled-coil tag−probe method[9]. This labeling method could overcome the problems of the conventional methods and correctly determine the oligomeric states of monomeric, dimeric, and tetrameric membrane proteins.

Chapter 2

Oligomeric state of β_2-adrenergic receptor

2.1 Introduction

G-protein-coupled receptors (GPCRs) are known as seven-transmembrane receptors, which transduce many important physiological signals and are targets for a large fraction of therapeutic drugs[30]. Recently, oligomerization of GPCRs has been a topic of broad interest because of its functional relevance and potential importance in development of new drugs[31,32]. However, significant controversy exists on oligomeric states of GPCRs, as for β_2-adorenergic receptor (β_2AR)[4,5,6,7,33,34], although it is the subtype of family A receptors. The discrepancy in existing approaches are due to the lack of precise way to stoichiometrically determine oligomeric states of membrane proteins on living cells; firstly, fusion proteins with fluorescent or luminescent proteins (~27 kDa) with BRET methods have functional limitations as stated in Chapter 1; secondly, overexpression may raise artificial oligomerization and/or random transfer; thirdly, FRET or BRET methods were not validated using standard membrane proteins. In addition, it is also important to investigate not only oligomeric states of membrane proteins on living cells but also their functional relevance.

To improve such a situation, I examined the oligomeric state of β_2ARs with FRET to clarify its functional relationship using the coiled-coil tag−probe labeling technique[9] combined with spectral imaging. I found that β_2ARs could transduce cyclic AMP (cAMP) signals in two cell lines without showing any FRET signals. Thus, β_2ARs do not form constitutive homooligomers, and homooligomerization is not necessary for the receptor function of β_2ARs.

2-2 Materials and Methods

Vector construct.

For stable-expression of E3-tagged human β_2AR (E3-β_2AR), cDNA encoding E3-β_2AR was inserted into a pcDNA5/FRT vector[12] (Life Technology, Carlsbad, US).

For transient expression, cDNA encoding E3-β_2AR was inserted into pcDNA3 (Life Technology, Carlsbad, US) as follows. The gene of β_2AR, which had a *Nhe*I site at the 5'-terminus, an *Apa*I site at the 3'-terminus, and a stop codon before the *Apa*I site, was amplified by PCR from E3-β_2AR-EYFP/pcDNA3 and the product were digested with *Nhe*I and *Apa*I to acquire insert DNA for β_2AR. E3-EP3β/pcDNA3 vector were digested with *Nhe*I and *Apa*I to obtain vector DNA (E3/pcDNA3). The DNA for β_2AR was then inserted into the vector DNA (E3/pcDNA3) to obtain an E3-β_2AR/pcDNA3 vector.

Cell culture.

Flp-in CHO cells (Life Technology, Carlsbad, US) and CHO-K1 cells were used for stable expression and transient expression of membrane proteins, respectively. Both CHO cells were cultured in Ham's F12 medium supplemented with 10% FBS, L-glutamine and antibiotics at 37°C in a 5% CO_2 incubator (Sanyo Electric Co., Ltd., Osaka, Japan). Hygromycin at 500 μg/mL (Nacalai Tesque, Kyoto, Japan) was used for Flp-in CHO cells, and penicillin at 50 units/mL and streptomycin at 50 μg/mL (Nacalai Tesque, Kyoto, Japan) were used for CHO-K1 cells. HEK293 cells were cultured in DMEM (4.5 mg/mL of glucose) supplemented with 10% FBS, L-glutamine, and antibiotics of penicillin at 50 units/mL and streptomycin at 50 μg/mL (Nacalai Tesque, Kyoto, Japan).

Transfection.

Previously, I constructed E3-tagged human β_2AR stably-expressing CHO cells (E3-β_2AR-CHO (stable))[12]. The cells was seeded at 3.0×10^5/dish in a 35-mm glass bottom dish ((Advanced TC treated), Greiner bio-one, Kremsmüenster, Austria), and imaged at 24−36 h from seeding. For transfection into CHO-K1 cells, refer Materials and Methods in Chapter 1. HEK293 cells were seeded at 1.0×10^5 in a glass bottom dish. The medium for HEK293 cells was carefully changed to a fresh medium containing 10% FBS, and the cells were incubated with a transfection mixture composed of 2.0 μg of DNA, 4.0 μL of Lipofectamine LTX (Life Technology, Carlsbad, US), and 400 μL of Opti-MEM (Life Technology, Carlsbad, US) per dish at 30 h from

seeding without the second medium change after transfection, because repeated medium change might detach HEK293 cells from the dish. HEK293 cells were imaged at 18 h from transfection. For transfection of E3-mGluR1b, the transfection mixture was composed of 2.0 μg of DNA, 8.0 μL of Lipofectamine LTX, 2.0 μL of PLUS reagent (Life Technology, Carlsbad, US), and 400 μL of Opti-MEM per dish.

Examining homooligomerization of E3-β_2AR stimulated with ligands.

When E3-β_2AR was labeled with treatment with ligands, the receptors were labeled with 50 nM K4 probe solutions (1 mL) for 2 min, and then stimulated with mixtures of doubly concentrated ligands (1 mL) containing 50 nM K4 probes. The final concentration of isoproterenol (Sigma, Buchs, Switzerland) and timolol (Sigma) was 10 μM and that of carazolol (Wako, Saitama, Japan) and ICI118,551 (Sigma) was 1 μM. The stimulation of β_2ARs by isoproterenol was for 30 min and that by the other ligands, 10 min.

cAMP assay.

I measured cAMP concentrations using an AlphaScreen^{TM} cAMP assay kit (Perkin elmer, Waltham, US) according to the manufacturer's instructions, except that the Donor beads in lysis buffer were added to cells before the Acceptor beads in stimulation buffer because the lysis of cell membranes is required for stimulation with isoproterenol to cease when assaying the changes in time-dependent cAMP responses. Briefly, for the cAMP assay of E3-β_2AR-CHO (stable), the cells were seeded in a 384-well plate at 1,000 cells per well at 24 h from seeding. For the cAMP assay of E3-β_2AR-HEK293 (transient), cells were seeded at 2,500 cells per well at 18 h from transfection because the transfection efficiency of E3-β_2ARs was 40−50% as judged from confocal images (data not shown). For determining EC_{50} values, the HEK293 and CHO cells were incubated with isoproterenol at 10^{-15} to 10^{-4} M for 30 min at 30°C. For assaying time-dependent cAMP responses, the HEK293 cells were incubated with isoproterenol at 10 μM for 0, 5, 10, 15, 20, and 25 min. The cAMP responses were fitted to

$$Y = Bottom + \frac{Top - Bottom}{1 + 10^{(LogX - LogEC_{50})}} \qquad \text{[Eq. 4]}$$

where Y represents the concentration of cAMP, X denotes the concentration of isoproterenol, Top indicates the top asymptote of the curve corresponding to the total binding of acceptor beads to cellular cAMP, and Bottom means the bottom asymptote of the curve corresponding to the total binding of acceptor beads to biotinylated cAMP.[14]

Crosslinking β_2AR with antibody and Protein A.

Anti-N-terminus (7−37 residues) β_2AR rabbit polyclonal antibodies (5.0 μg / mL) (Abgent) in 1 mL of PBS (+) were added to the cells and incubated for 30 min at 37°C. After incubation of the antibodies, the solutions were removed. A mixture of K4 probes at X_D = 0.74 and Protein A (1.0 μg / mL) (Life Technology, Carlsbad, US) in 1 mL of PBS (+) was then added to the cells and incubated for 5 min at 37°C before imaging.

Identification of expression level of E3-β_2AR-CHO (stable).

The expression level (1.3 ± 0.2 × 10^5 receptors / cell) of E3-β_2AR-CHO (stable) has been previously determined by [^{3}H] CGP-12177[12,35], and equals 66 receptors / μm^2 assuming a cell diameter of 25 μm (n = 58). According to a previous report[5] (2.4 × 10^4 receptors / μm^2 ≅ 47 pmol / mg protein), 66 receptors / μm^2 corresponds to 1.3 × 10^{-1} pmol / mg protein, which was comparable to those of human heart tissue[5,36] (~0.8 × 10^{-1} pmol / mg protein) and dog heart tissue[5] (~3.0 × 10^{-1} pmol / mg protein).

2.3 Results

Expression level, folding, and functional activity of E3-β_2AR on CHO cells.

Although β_2AR is one of the best studied membrane receptors, it is controversial whether oligomerization of β_2ARs is required for signaling on living cells[33,34]. I confirmed that CHO cells did not express detectable levels of endogenous β_2ARs based on a cAMP assay (data not shown). Hence, FRET signals from E3-β_2ARs on host CHO cells should directly reflect their homooligomeric states without forming oligomers with endogenous β_2ARs. I determined the state of β_2ARs at a fixed X_D value of 0.74 because the E_{app} value is sensitive to the oligomeric states of membrane proteins at the X_D value (**Fig. 1-3B**). Larger differences in E_{app} are obtained at larger X_D values. However, weaker emission due to a lower concentration of acceptor can result in a larger experimental error. So, I adopted X_D = 0.74 to achieve a good balance between accuracy and sensitivity. The expression level of E3-β_2ARs stably expressed on CHO cells (E3-β_2AR-CHO (stable)) was determined by using the radioactive isotope ligand [^{3}H] CGP-12177. The average level ($1.3 \pm 0.2 \times 10^5$ receptors / cell) was comparable to that reported for human and dog heart tissues (see Methods in Chapter 2), and much less than that of a previous report in which β_2ARs were overexpressed at 3.8–32.9 fold physiological levels[5]. I also confirmed that E3-tagged β_2ARs were correctly folded and fully functional. The degree of receptor internalization upon agonist stimulation quantified from confocal images for the receptors labeled by the coiled-coil method (42 ± 4%, **Fig. 2-1A**) was in good agreement with that estimated using [^{3}H] CGP-12177 (40 ± 6%). Furthermore, the receptors exhibited cAMP responses on treatment with isoproterenol in a dose-dependent manner with an EC_{50} value of 3.0×10^{-10} M (**Fig. 2-1B**), which was comparable with a reported value of 5.6×10^{-10} M for β_2AR[37].

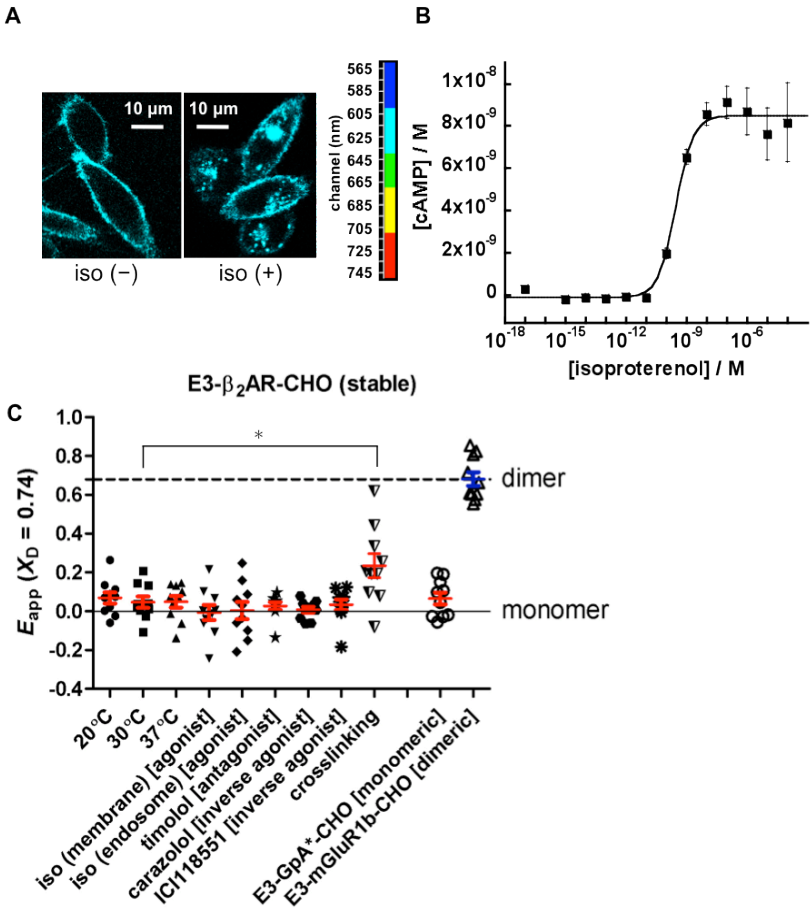

Figure 2-1. Self-association and receptor function of E3-β_2AR-CHO (stable). (A) Spectral images for E3-β_2AR-CHO (stable) without (left) and with (right) treatment with 10 μM isoproterenol (iso) for 30 min at 30°C after labeling with K4 probes. Granular bright spots after iso stimulation indicate the internalized receptors from the cell surface. Images are shown in pseudo-color (the scale bar on the right). These images are composite of 19 channels in the range of 565 to 745 nm (resolution: 10 nm). (B) The cAMP response of E3-β_2AR-CHO (stable) on treatment with isoproterenol at 30°C. Error bars represent the mean ± s.e.m., $n = 3$. (C) The E_{app} values for E3-β_2AR-CHO (stable), E3-GpA*-CHO (transient), and E3-mGluR1b-CHO (transient) labeled with K4 probes at $X_D = 0.74$. Iso (membrane) and iso (endosome) denote the E_{app} values on plasma membranes and endosomes after treatment with the agonist isoproternol, respectively. The antagonist timolol, the inverse agonists carazolol and ICI118551 were also administrated and the E_{app} values were determined on plasma membranes. The dotted line shows the average E_{app} value (0.68) for 100% dimers, assuming $E = 1$. Error bars represent the mean ± s.e.m., $n = 10$. * $P < 0.05$ (two-tailed Student's t test).

Oligomeric state of β_2AR on CHO cells and its functional relevance.

The Förster distance (R_0) of donor−acceptor pair (82 Å) covers the maximal plausible distance between the N-termini of a β_2AR dimer (~80 Å)[38], giving a minimal FRET efficiency of 54%, although a study in model lipid bilayers suggests that the transmembrane helix 1 close to the labeling site is an interface between β_2AR protomers[38]. I detected FRET signals of E3-β_2AR-CHO (stable) at temperature-controlled environments because the previous experiments were performed at various temperatures[7,38,39]. E_{app} variances for E3-β_2AR-CHO (stable) at 20, 30, and 37°C without treatment with ligands were indistinguishable from that for monomeric GpA* (**Fig. 2-1**). The variances were not derived from the partial oligomerization because10–20% dispersions were observed even in the standard membrane proteins (0.68 ± 0.11 for dimeric E3-mGluR1b-CHO and 0.07 ± 0.10 for monomeric E3-GpA*-CHO). In the ligand treatment experiments, temperature was set at 30°C because internalization of E3-β_2ARs was significant at 37°C. Although E_{app} values after stimulation with a β_2AR agonist (isoproterenol) appear to be more dispersed, the average values for plasma membranes and endosomes were 0.00 ± 0.12 and 0.00 ± 0.14, respectively. Even after stimulation with an antagonist (timolol) and inverse agonists (carazolol and ICI118,551), no increase in E_{app} was observed (**Fig. 2-1**). In contrast, crosslinking of the receptors by treatment with bivalent anti-β_2AR primary antibody and Protein A resulted in an increase in E_{app}, indicating that if β_2ARs form oligomers, significant FRET signals should be observed (see also **Fig. 2-3**). Furthermore, the E_{app} values of crosslinked β_2ARs were smaller than those of E3-mGluR1b (dimer), suggesting that E3-β_2ARs expressed on CHO cells were rather separated with each other on the cell surfaces, therefore only partially crosslinked. This is also supported by the recent report using photoactivated localization microscopy that β_2AR does not cluster in fixed CHO cells[40]. The average distance between monomeric β_2ARs is approximately 1,400 Å based on the cell surface area per receptor, assuming a globular shape of the cell with a diameter of 25 μm.

To check the effect of the expression method and host cell, I also performed FRET experiments for E3-β_2ARs transiently expressed on CHO cells (E3-β_2AR-CHO (transient)). I found that E3-β_2AR-CHO (transient) did not show any FRET signals under various conditions (**Fig. 2-2**).

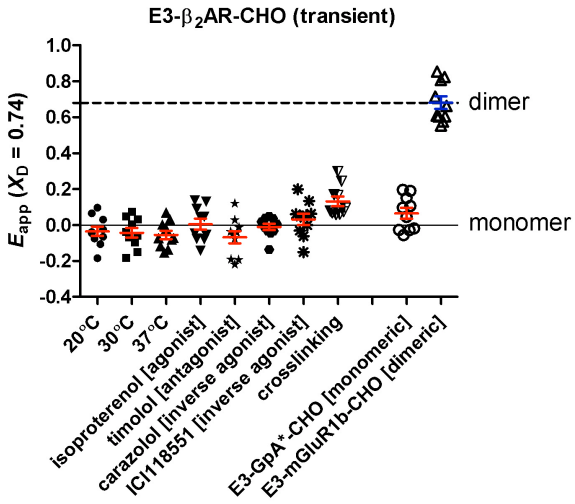

Figure 2-2. Self-association of E3-β$_2$AR-CHO (transient). The E_{app} values for E3-β$_2$AR-CHO (transient), E3-GpA*-CHO (transient) (monomeric standard), and E3-mGluR1b-CHO (transient) (dimeric standard) labeled with K4 probes at X_D = 0.74. The dotted line shows the average E_{app} value (0.68) for 100% dimers, assuming E = 1. The E_{app} values on plasma membranes were measured at various temperatures (20, 30, 37°C) without and with treatment with ligands (the agonist isoproterenol, the antagonist timolol, the inverse agonists carazolol and ICI118551) at 30°C. Anti-β$_2$AR (N-terminus) polyclonal antibodies and Protein A were used for the crosslinking experiment. Error bars represent the mean ± s.e.m., n = 10. ** $P < 0.01$ (two-tailed Student's t test).

Oligomeric state of β_2AR on HEK293 cells and its functional relevance.

In previous reports, oligomerization of β_2ARs has been measured by using receptors transiently expressed in human embryonic kidney (HEK293) cells[4,5,6]. So, I also performed same experiments with E3-β_2ARs transiently expressed on HEK293 cells (E3-β_2AR-HEK293 (transient)). Again, no significant FRET signals were detected for E3-β_2AR-HEK293 (transient) at 20, 30, and 37°C without treatment with ligands (**Fig. 2-3A**). In contrast, on treatment with ligands, especially with isoproterenol, slight increases in FRET signals were observed (**Fig. 2-3A**). The average E_{app} for isoproterenol-treated receptors was 0.27 and one value was comparable to that for 100% dimer. However, the true E_{app} value should be larger because heterooligomerization between E3-β_2ARs and endogenous β_2ARs on HEK293 cells[2] do not give FRET signals. I estimated that the upper limit of the expression level of endogenous β_2ARs was ~1 / 3.8 of that of E3-β_2ARs from the maximum production level of cAMP (**Fig. 2-3B**), assuming that the cAMP response is proportional to the expression level.

I tried to clarify the reason of increase in FRET signals. To examine the possibility of an increase in FRET signals through domain concentration, membrane cholesterol was depleted by treatment with compactin or metyl-β-cyclodextrin. However, I did not observe any decrease in FRET signals (data not shown). The local accumulation of β_2ARs in the plasma membranes observed in 10–25 min after stimulation (the yellow arrows in **Fig. 2-3D**) might indicate the oligomerization of the receptors. However, there was no correlation between E_{app} values and fluorescence intensity (proportional to the expression level) on the membrane. These results demonstrate the increased FRET signals result from neither the domain concentration nor the local accumulation.

On the other hands, I found that initiation of the increase in FRET signals (15 min) was significantly delayed compared with that of cAMP production and internalization (5 min) ($p < 0.01$, two-tailed Student's t test) (**Figs. 2-3C and D**). The above observation indicates that the increased E_{app} values are post-signaling oligomerization, which may be driven by cell-dependent unknown mechanisms. I concluded that homooligomerization of β_2ARs were also not necessary for functions on HEK293 cells.

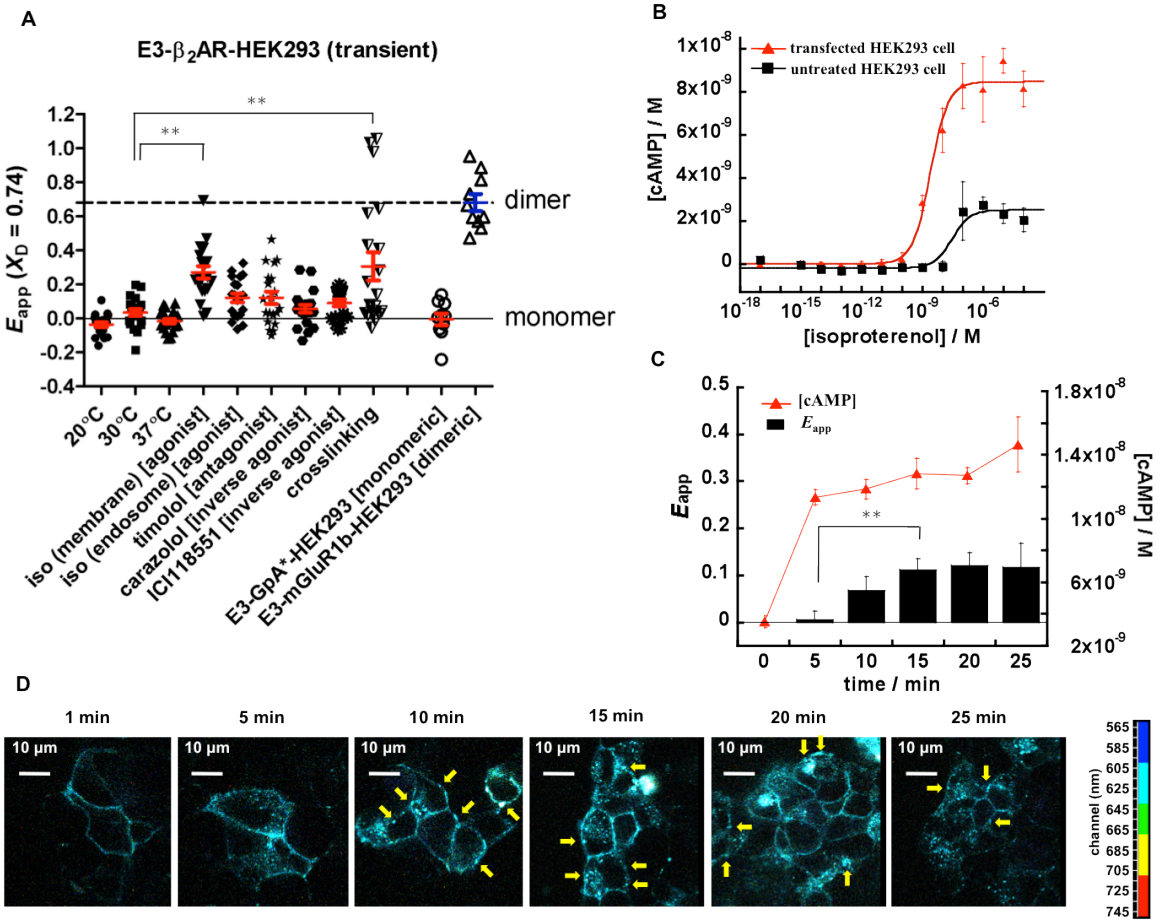

Figure 2-3. Relationship between oligomerization and function of E3-β_2AR-HEK293 (transient). (A) The E_{app} values for E3-β_2AR-HEK293 (transient), E3-GpA*-HEK293 (transient), and E3-mGluR1b-HEK293 (transient) labeled at $X_D = 0.74$. Similar experiments to figures 2-1 and 2-2 were performed using E3-β_2ARs transiently expressed on HEK293 cells. Error bars represent the mean ± s.e.m., $n = 20$ (β_2AR) and $n = 10$ (GpA*, mGluR1b). ** $P < 0.01$ (two-tailed Student's t test). (B) cAMP response of E3-β_2AR-HEK293 (transient) on treatment with isoproterenol at 30°C. Error bars represent the mean ± s.e.m., $n = 3$. (C) Time course of FRET increase and cAMP production for E3-β_2AR-HEK293 (transient) treated with 10 μM isoproterenol. Error bars represent the mean ± s.e.m., $n = 10$ (E_{app}) and $n = 3$ (cAMP assay). ** $P < 0.01$ (two-tailed Student's t test). (D) The spectral images of internalization of E3-β_2AR-HEK293 (transient) after stimulation with 10 μM isoproterenol. Images are shown in pseudo-color (the scale bar on the right). These images are composite of 19 channels in the range of 565 to 745 nm (resolution: 10 nm). The yellow arrows indicate the regions of locally accumulated β_2ARs on the membranes.

2.4 Discussion

There is currently dispute over oligomerization of β_2AR, a typical family A GPCR, on living cells. James *et al*. concluded that β_2AR did not form dimer and pointed out the possibility that the actual amounts of dimers might be limited at a physiological expression level[6], whereas Mercier *et al.* reported that more than 80% of β_1AR and β_2AR formed constitutive homo- and heterodimers and that the dimerization is insensitive to receptor density[5]. The difference between their interpretations has developed into a major controversy[33,34]. Meanwhile, Dorsch *et al.* demonstrated that β_2ARs form stable oligomers on living cells by using fluorescence recovery after photobleaching method, in which the target proteins fused with YFP at the extracellular region were immobilized with polyclonal antibodies and then the lateral mobility of the nonimmobilized fraction fused with CFP at the intracellular region was determined[39].

This long-standing debate is due to the lack of methods for easy and precise detection of oligomeric state of membrane proteins on living cells as described. In the present study, I used the coiled-coil labeling method to overcome the problems of the fusion proteins and found that β_2ARs on the cell surface do not form constitutive homooligomers regardless of the cell species and method for expression, and that they exist as monomers or may form heterooligomers with other receptors[41,42,43]. On the other hand, they showed cAMP responses and internalization on treatment with isoproterenol, demonstrating that homooligomerization is not necessary for the receptor functions of β_2ARs. These results are consistent with the in vitro observation that a monomeric β_2AR is the minimal functional unit necessary for signaling[43]. Moreover, Scarselli *et al*. also recently found that β_2AR does not cluster in fixed CHO cells by using photoactivated localization microscopy[40]. Note that the absence of FRET signals did not originate from defects in the experimental system because treatments with the crosslinkers antibodies and Protein A on the agonist isoproterenol resulted in a significant increase in E_{app}, indicating that our method can detect the association between β_2ARs when they form oligomers.

Our results in this study with stoichiometric analysis provide a final solution to the long-standing debate about the oligomeric state of β_2AR for a decade. Using the coiled-coil tag−probe labeling method combined with spectral imaging, I investigated the relationship between oligomeric states of β_2AR and its functions after having confirmed that the E3-tagged receptors were fully functional, and found that β_2ARs on the cell surface do not form constitutive homooligomers regardless of the cell species and method for expression.

Chapter 3

Oligomeric state of M2 proton channel of influenza A virus

Section 1

Oligomeric state of wild-type M2 proton channel

3.1 Summary

When influenza A virus infects host cells, its integral matrix protein M2 forms a proton-selective channel in the viral envelope. Although X-ray crystallography and NMR studies using fragment peptides have suggested that M2 stably forms a tetrameric channel irrespective of pH, the oligomeric states of the full-length protein in living cells have not yet been clarified. In the present study, I utilized the stoichiometric analytical method established in Chapter 1 to examine the relationship between the oligomeric states of full-length M2 and its channel activities in living cells. In contrast to previous models, M2 formed proton-conducting dimers at neutral pH and these dimers were reversibly converted to tetramers at acidic pH. The H37A and W41A mutants exhibited only the dimeric FRET signals at pH 4.9, indicating that the cation-π interaction between the His37 and Trp41 residues plays the role in the driving force of tetramerization. The antiviral drug amantadine hydrochloride (Am) inhibited both tetramerization and channel activity.

To elucidate the mechanism by which the dimeric form displayed the channel activity, I performed the alanine-scanning against the transmembrane region of the full-length M2 protein at pH 6.0. As a result, the channel activities of the H37A and I35A mutants were significantly decreased (approximately 35- and 10-fold decrease compared with WT, respectively), whereas their oligomeric states were not affected. I, therefore, predicted that Ile35–choresterol interaction is required for the dimer function. The removal of cholesterol resulted in a significant decrease in the activity of the dimer. These results indicate that the minimum functional unit of the M2 protein is a dimer, which forms a complex with cholesterol for its function.

Chapter 3

Oligomeric state of M2 proton channel of influenza A virus

Section 2

Oligomeric state of the amantadine-resistant S31N mutant of M2 proton channel

3.2 Summary

The integral matrix protein M2 of influenza A virus has been proposed to form a proton-selective channel and is the target of the antiviral drug amantadine hydrochloride (Am). A significant increase in Am-resistant strains containing the predominant S31N mutation in the M2 protein has been reported. By using the FRET analysis method, I examined the oligomeric state of the S31N mutant. I revealed that the S31N mutant predominantly formed a proton-permeable dimer irrespective of pH. It is surprising, but this was consistent with the result that similar channel activities at pH 6.0 and 4.9 were observed, whereas WT exhibited the different activities dependent on pH. The S31L mutant also exhibited a dimeric FRET signal, but the S31Q and S31A mutants displayed tetrameric signals at pH 4.9, demonstrating that the length of the 31st side chain is important for stabilization of the dimeric form. On the other hand, the S31L mutant lost the channel activity as opposed to the S31N mutant, indicating that the 31st amino acid of M2 channel is involved in conducting protons in the dimeric state. The hydrophobic side chain of leucine causes a cessation of proton permeation because it is not responsible for proton relay. In the presence of 100 μM Am, the channel activity of the E3-S31A mutant was completely inhibited, whereas that of the S31Q mutant was retained. Taken together, these results indicated that the length and the presence of an amide group of the 31st side chain are significant for stabilization of the dimeric form and acquisition of Am resistance, respectively. The S31N mutant combines the appropriate length and the property to be suitable for formation of a drug-ineffective rigid dimer.

Summary

Perspectives

Publications

Acknowledgements

References

Summary

Not only conformational changes but also the oligomeric states of membrane proteins are proposed to modulate their functions. However, existing methodologies are not suitable to quantitatively analyze the oligomeric states of membrane proteins in living cells.

In Chapter 1, I combined the coiled-coil tag–probe labeling technology and spectral imaging to establish the stoichiometric analysis of the oligomeric states of membrane proteins in living cells using monomeric, dimeric, and tetrameric standard proteins.

In Chapter 2, I examined the oligomeric state of β_2AR, which has been significantly controversial for a decade although β_2AR is a well-known subtype of family A GPCR. I found that β_2AR could transduce cAMP signals and be internalized in CHO cells without showing any FRET signals irrespective of expression methods (stable or transient). β_2AR in HEK293 cells slightly exhibited FRET signals on treatment with isoproterenol; however, the initiation of increase in FRET signal was delayed compared with those of cAMP production and internalization. These results demonstrate that β_2AR on the cell surface do not form constitutive homooligomers regardless of cell species and methods of expression.

In Section 1 of Chapter 3, I investigated the oligomeric state of WT M2 proton channel of influenza A virus. While the vast majority of research groups consider that M2 exists as a stable tetramer using fragment peptides incorporated into artificial environments, dynamic equilibrium between the oligomeric states of the full-length M2 protein in biomembranes has never been examined. I revealed pH-dependent dimer−tetramer transition of M2 in living cells for the first time. Furthermore, the dimeric form of M2 protein exhibited channel activity; therefore I proposed a functional dimer model. The results in this section revealed that the full-length protein behaves different from the fragment peptides and that physiological conditions including lipid environments surrounding the proteins are very important for elucidation of the structures and their functional relevance.

In Section 2 of Chapter 3, I also examined the oligomeric state of the Am-resistant S31N M2 channel. Surprisingly, the S31N mutant displayed dimeric FRET signal and similar channel activities irrespective of pH and the presence of Am, as opposed to WT. However, the channel activity was more than 4-fold decreased compared with WT, indicating that the mutation from serine to asparagine in the 31st position is suitable for Am resistance but not effective for proton conduction.

Perspectives

The native behaviors of target proteins under the physiological condition are not easy to be investigated. The researchers would be unable to escape sacrificing more or less natural conditions and states in which the proteins should be as long as they specifically investigate a particular protein in the simplified experimental systems. For example, once you attach a tag to the protein for labeling, the tagged protein is not native state at the time. This is not confined to our coiled-coil labeling method, but is a common issue in any methodologies. What is important is firstly to check the absence of influence of tagging on the function or the structure of the target protein and to perform experiments under the native condition as much as possible throughout the study.

In these studies, I demonstrated that our less perturbing methodology is a powerful tool for analyzing not only oligomeric states of membrane proteins on living cells but also their functional relevance, as exemplified by β_2AR. Moreover, the findings of oligomeric states of M2 proteins propose a new approach for elucidation of resistance mechanism for adamantane-based drugs and discovery of a novel drug with different mode of action in future works.

I also want to develop my work into the native oligomeric states of endogenously expressing membrane proteins. For example, I plan to label the endogenous β_2ARs in cells and tissues with donor and acceptor fluorescent ligands to analysis the oligomeric state (**Supplementary Figure 1**), and compare the result with those in the transfected cells. E3-β_2ARs are used as a positive control after labeled with donor fluorescent K4 probes and acceptor fluorescent ligands at the same time (**Supplementary Figure 1**). Although this method has a 'restriction' that the oligomeric state reflects the condition when endogenous β_2ARs are stimulated by the ligands and the structure without stimulation remains unclear, this strategy makes it possible to detect the native oligomerization of intact β_2AR under the physiological condition.

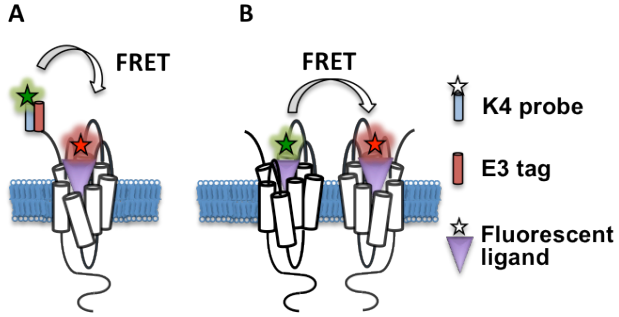

Figure S-1. The diagram to detect the FRET signal for endogenous β_2ARs. (A) Inevitable intermolecular FRET in one E3-β_2AR labeled with the different methods used for the positive control. (B) The image of FRET between endogenous β_2ARs labeled with donor and acceptor fluorescent ligands.

I think it is not impossible to measure the FRET signal of M2 protein on the envelope of influenza A virus. The diameter of spherical virus is ~100 nm, which is comparable to that of small unilamellar vesicle. Previously, our laboratory's members established the measurement of ensemble FRET of fluorescent-labeled single-pass trasmembrane peptides incorporated into the vesicle; therefore, the detection of FRET for the genetically-transformed E3-tagged M2 protein is theoretically feasible study. Although I found out the dynamic equilibrium between dimer–tetramer of WT M2 protein on living cells, the true oligomeric state on the viral envelope remain unclear. The density of expressing proteins on the envelope and curvature of viral particle might be different with the condition of living cells. Thus, investigation of the native oligomeric state of M2 protein on the virus is also an important theme.

Publications

1. Yano, Y., Kawano, K., Omae, K. & Matsuzaki, K. (2012)
Coiled-Coil Tag–Probe Labeling Methods for Live-Cell Imaging of Membrane Receptors.
Methods in Enzymology 504, 355–369.

2. Kawano, K., Yano, Y., Omae, K., Matsuzaki, S. & Matsuzaki, K. (2013)
Stoichiometric analysis of oligomerization of membrane proteins on living cells using coiled-coil labeling and spectral imaging.
Analytical Chemistry 85, 3454–3461.

3. Kawano, K., Yano, Y. & Matsuzaki, K. (2014)
A Dimer is the Minimal Proton-Conducting Unit of the Influenza A Virus M2 Channel.
(under submission)

4. Kawano, K., Yano, Y. & Matsuzaki, K. (2014)
Steady Dimer Formation by the Amantadine-Resistant S31N Mutant of Influenza A Virus M2 Protein.
(to be submitted)

Acknowledgements

I would like to express here my deep and sincere gratitude to Professor Katsumi Matsuzaki (Graduate School of Pharmaceutical Sciences, Kyoto University) for providing me the significant guidance about the present study and opening the path for me to enter the biophysical field in academia.

I would like to extend appreciation for Assistant Professor Yoshiaki Yano (Graduate School of Pharmaceutical Sciences, Kyoto University) for consistently giving me courteous guidance and technical advice throughout the study. He well cares and occasionally admonished with gentleness for me.

I am deeply grateful to Associate Professor Masaru Hoshino (Graduate School of Pharmaceutical Sciences, Kyoto University) for his helpful advice and suggestions.

Thanks to these leaders, I am absolutely fascinated with research. I would never have been today without their empathetic supports.

I am also obliged to Professor Nobutaka Fujii and Instructor Shinya Oishi (Graduate School of Pharmaceutical Sciences, Kyoto University) for technical advice on peptide synthesis in Chapter 1, Assistant Professor Rinshi Kasai (Institute of Integrated Cell-Material Sciences (iCeMS), Kyoto University) for useful discussion on the oligomeric state of β_2AR in Chapter 2, and Associate Professor Tyuji Hoshino (Graduate School of Pharmaceutical Sciences, Chiba University) for helpful suggestion on the oligomeric state of M2 proton channel in Chapter 3.

I had a great opportunity to research with a nice group of people in my laboratory, Department of Biophysical Chemistry, Graduate School of Pharmaceutical Sciences, Kyoto University. I deeply thank everyone.

Finally, I would like to express my grateful acknowledgement to my wife Mika Kawano and my mother Reiko Kawano for their committed supports.

References

1. Bockaert, J. & Pin, J. P. (1999). Molecular tinkering of G protein-coupled receptors: an evolutionary success. EMBO J. 18, 1723-1729.
2. Jordan, B. A. & Devi, L. A. (1999). G-protein-coupled receptor heterodimerization modulates receptor function. Nature 399, 697-700.
3. Michineau, S., Alhenc-Gelas, F. & Rajerison, R. M. (2006). Human bradykinin B2 receptor sialylation and N-glycosylation participate with disulfide bonding in surface receptor dimerization. Biochemistry 45, 2699-2707.
4. Angers, S., Salahpour, A., Joly, E., Hilairet, S., Chelsky, D., Dennis, M. & Bouvier, M. (2000). Detection of β_2-adrenergic receptor dimerization in living cells using bioluminescence resonance energy transfer (BRET). Proc. Natl. Acad. Sci. USA 97, 3684-3689.
5. Mercier, J. F., Salahpour, A., Angers, S., Breit, A. & Bouvier, M. (2002). Quantitative assessment of β_1- and β_2-adrenergic receptor homo- and heterodimerization by bioluminescence resonance energy transfer. J. Biol. Chem. 277, 44925-44931.
6. James, J. R., Oliveira, M. I., Carmo, A. M., Iaboni, A. & Davis, S. J. (2006). A rigorous experimental framework for detecting protein oligomerization using bioluminescence resonance energy transfer. Nat. Methods 3, 1001-1006.
7. Maurel, D., Comps-Agrar, L., Brock, C., Rives, M. L., Bourrier, E., Ayoub, M. A., Bazin, H., Tinel, N., Durroux, T., Prezeau, L., Trinquet, E. & Pin, J. P. (2008). Cell-surface protein-protein interaction analysis with time-resolved FRET and snap-tag technologies: application to GPCR oligomerization. Nat. Methods 5, 561-567.
8. George, N., Pick, H., Vogel, H., Johnsson, N. & Johnsson, K. (2004). Specific labeling of cell surface proteins with chemically diverse compounds. J. Am. Chem. Soc. 126, 8896-8897.
9. Yano, Y., Yano, A., Oishi, S., Sugimoto, Y., Tsujimoto, G., Fujii, N. & Matsuzaki, K. (2008). Coiled-coil tag–probe system for quick labeling of membrane receptors in living cell. ACS Chem. Biol. 3, 341-345.
10. Meyer, B. H., Segura, J. M., Martinez, K. L., Hovius, R., George, N., Johnsson, K. & Vogel, H. (2006). FRET imaging reveals that functional neurokinin-1 receptors are monomeric and reside in membrane microdomains of live cells. Proc. Natl. Acad. Sci. USA 103, 2138-2143.
11. Fairclough, R. H. & Cantor, C. R. (1978). The use of singlet-singlet energy transfer to study macromolecular assemblies. Methods Enzymol. 48, 347-379.
12. Yano, Y. & Matsuzaki, K. (2011). Fluorescence ratiometric detection of ligand-induced receptor internalization using extracellular coiled-coil tag–probe labeling. FEBS Lett. 585, 2385-2388.
13. Litowski, J. R. & Hodges, R. S. (2002). Designing heterodimeric two-stranded α-helical coiled-coils. Effects of hydrophobicity and α-helical propensity on protein folding, stability, and specificity. J. Biol. Chem. 277, 37272-37279.
14. Deupi, X. (2013). Relevance of rhodopsin studies for GPCR activation (in press). Biochim. Biophys. Acta.
15. Stouffer, A. L., Acharya, R., Salom, D., Levine, A. S., Di Costanzo, L., Soto, C.

S., Tereshko, V., Nanda, V., Stayrook, S. & DeGrado, W. F. (2008). Structural basis for the function and inhibition of an influenza virus proton channel. Nature 451, 596-599.
16. Doumazane, E., Scholler, P., Zwier, J. M., Trinquet, E., Rondard, P. & Pin, J. P. (2011). A new approach to analyze cell surface protein complexes reveals specific heterodimeric metabotropic glutamate receptors. FASEB J. 25, 66-77.
17. Duong, M. T., Jaszewski, T. M., Fleming, K. G. & MacKenzie, K. R. (2007). Changes in apparent free energy of helix-helix dimerization in a biological membrane due to point mutations. J. Mol. Biol. 371, 422-434.
18. Herrick-Davis, K., Grinde, E., Lindsley, T., Cowan, A. & Mazurkiewicz, J. E. (2012). Oligomer size of the serotonin 5-hydroxytryptamine 2C (5-HT2C) receptor revealed by fluorescence correlation spectroscopy with photon counting histogram analysis: evidence for homodimers without monomers or tetramers. J. Biol. Chem. 287, 23604-23614.
19. Ulbrich, M. H. & Isacoff, E. Y. (2007). Subunit counting in membrane-bound proteins. Nat. Methods 4, 319-321.
20. Kasai, R. S., Suzuki, K. G., Prossnitz, E. R., Koyama-Honda, I., Nakada, C., Fujiwara, T. K. & Kusumi, A. (2011). Full characterization of GPCR monomer-dimer dynamic equilibrium by single molecule imaging. J. Cell Biol. 192, 463-480.
21. Hern, J. A., Baig, A. H., Mashanov, G. I., Birdsall, B., Corrie, J. E., Lazareno, S., Molloy, J. E. & Birdsall, N. J. (2010). Formation and dissociation of M1 muscarinic receptor dimers seen by total internal reflection fluorescence imaging of single molecules. Proc. Natl. Acad. Sci. USA 107, 2693-2698.
22. Guo, W., Urizar, E., Kralikova, M., Mobarec, J. C., Shi, L., Filizola, M. & Javitch, J. A. (2008). Dopamine D2 receptors form higher order oligomers at physiological expression levels. EMBO J. 27, 2293-2304.
23. Overton, M. C. & Blumer, K. J. (2000). G-protein-coupled receptors function as oligomers in vivo. Curr. Biol. 10, 341-344.
24. Hamatake, M., Aoki, T., Futahashi, Y., Urano, E., Yamamoto, N. & Komano, J. (2009). Ligand-independent higher-order multimerization of CXCR4, a G-protein-coupled chemokine receptor involved in targeted metastasis. Cancer. Sci. 100, 95-102.
25. Guignet, E. G., Hovius, R. & Vogel, H. (2004). Reversible site-selective labeling of membrane proteins in live cells. Nat. Biotechnol. 22, 440-444.
26. Yano, Y., Kawano, K., Omae, K. & Matsuzaki, K. (2012). Coiled-coil tag–probe labeling methods for live-cell imaging of membrane receptors. Methods Enzymol. 504, 355-370.
27. Yano, Y. & Matsuzaki, K. (2009). Tag–probe labeling methods for live-cell imaging of membrane proteins. Biochim. Biophys. Acta. 1788, 2124-2131.
28. Marti, D. N., Jelesarov, I. & Bosshard, H. R. (2000). Interhelical ion pairing in coiled coils: solution structure of a heterodimeric leucine zipper and determination of pK_a values of Glu side chains. Biochemistry 39, 12804-12818.
29. Zhu, L., Kemple, M. D., Yuan, P. & Prendergast, F. G. (1995). N-terminus and lysine side chain pK_a values of melittin in aqueous solutions and micellar dispersions measured by ^{15}N NMR. Biochemistry 34, 13196-13202.
30. Conn, P. J., Christopoulos, A. & Lindsley, C. W. (2009). Allosteric modulators

of GPCRs: a novel approach for the treatment of CNS disorders. Nat. Rev. Drug Discov. 8, 41-54.
31. Panetta, R. & Greenwood, M. T. (2008). Physiological relevance of GPCR oligomerization and its impact on drug discovery. Drug Discov. Today 13, 1059-1066.
32. Milligan, G. (2009). G protein-coupled receptor hetero-dimerization: contribution to pharmacology and function. Br. J. Pharmacol. 158, 5-14.
33. Bouvier, M., Heveker, N., Jockers, R., Marullo, S. & Milligan, G. (2007). BRET analysis of GPCR oligomerization: newer does not mean better. Nat. Methods 4, 3-4; author reply 4.
34. Salahpour, A. & Masri, B. (2007). Experimental challenge to a 'rigorous' BRET analysis of GPCR oligomerization. Nat. Methods 4, 599-600; author reply 601.
35. Koike, K. & Takayanagi, I. (1997). Characteristics of [^{3}H]CGP12177 binding sites at β_2- and β_3-adrenoceptors in the guinea pig taenia caecum. Gen. Pharmacol. 28, 73-76.
36. Steinfath, M., Danielsen, W., von der Leyen, H., Mende, U., Meyer, W., Neumann, J., Nose, M., Reich, T., Schmitz, W., Scholz, H. & et al. (1992). Reduced α_1- and β_2-adrenoceptor-mediated positive inotropic effects in human end-stage heart failure. Br. J. Pharmacol. 105, 463-469.
37. Elster, L., Elling, C. & Heding, A. (2007). Bioluminescence resonance energy transfer as a screening assay: Focus on partial and inverse agonism. J. Biomol. Screen. 12, 41-49.
38. Fung, J. J., Deupi, X., Pardo, L., Yao, X. J., Velez-Ruiz, G. A., Devree, B. T., Sunahara, R. K. & Kobilka, B. K. (2009). Ligand-regulated oligomerization of β_2-adrenoceptors in a model lipid bilayer. EMBO J. 28, 3315-3328.
39. Dorsch, S., Klotz, K. N., Engelhardt, S., Lohse, M. J. & Bunemann, M. (2009). Analysis of receptor oligomerization by FRAP microscopy. Nat. Methods 6, 225-230.
40. Scarselli, M., Annibale, P. & Radenovic, A. (2012). Cell type-specific β_2-adrenergic receptor clusters identified using photoactivated localization microscopy are not lipid raft related, but depend on actin cytoskeleton integrity. J. Biol. Chem. 287, 16768-16780.
41. Uberti, M. A., Hague, C., Oller, H., Minneman, K. P. & Hall, R. A. (2005). Heterodimerization with β_2-adrenergic receptors promotes surface expression and functional activity of α_{1D}-adrenergic receptors. J. Pharmacol. Exp. Ther. 313, 16-23.
42. McGraw, D. W., Mihlbachler, K. A., Schwarb, M. R., Rahman, F. F., Small, K. M., Almoosa, K. F. & Liggett, S. B. (2006). Airway smooth muscle prostaglandin-EP1 receptors directly modulate β_2-adrenergic receptors within a unique heterodimeric complex. J. Clin. Invest. 116, 1400-1409.
43. Whorton, M. R., Bokoch, M. P., Rasmussen, S. G., Huang, B., Zare, R. N., Kobilka, B. & Sunahara, R. K. (2007). A monomeric G protein-coupled receptor isolated in a high-density lipoprotein particle efficiently activates its G protein. Proc. Natl. Acad. Sci. USA 104, 7682-7687.